Journal of Thermal Analysis and Calorimetry (2019) 135:713–728
https://doi.org/10.1007/s10973-018-7394-5

Experimental investigation toward obtaining a new correlation for viscosity of WO_3 and Al_2O_3 nanoparticles-loaded nanofluid within aqueous and non-aqueous basefluids

Yaghoub Dehghani[1] · Ali Abdollahi[1] · Arash Karimipour[1]

Received: 5 February 2018 / Accepted: 17 May 2018 / Published online: 29 May 2018

Abstract
In this study, the effect of temperature and mass fraction of Al_2O_3 and WO_3 nanoparticles dispersed in deionized water and liquid paraffin was investigated on dynamic viscosity of nanofluid. The results of the TEM tests showed that the size of Al_2O_3 and WO_3 nanoparticles was ranged from 10 to 60 nm, and the results showed that nanoparticles were semi-spherical. Also the results of DLS and zeta potential tests, respectively, exhibited the uniform size and high stability of the nanoparticles in the basefluid environment. The findings showed that adding a certain amount of nanoparticles to water and liquid paraffin increases dynamic viscosity, and in the case of various shear rates, the viscosity is constant for the water-based nanofluids, which indicates the Newtonian behavior of the nanofluid. In addition, for those prepared by liquid paraffin as a basefluid, the viscosity does not remain constant at different shear rates and at low amount of shear rate the viscosity achieves higher value, indicating non-Newtonian behavior of liquid paraffin-based nanofluids. The results showed that by increasing the temperature in liquid paraffin-based nanofluid the uniformity and linearity of the viscosity curve at various shear rates could be observed, which represents an approach for Newtonian behavior of nanofluid at higher temperatures. These results also showed that with increasing the mass fraction of nanoparticles in water and liquid paraffin, the viscosity increases at different shear rates. Finally, the correlation presented in this study shows that for nanofluid viscosity as a function of nanoparticles load and temperature, the deviation of correlated data from experimental values is less than 10%.

Keywords Nanofluid · Dynamic viscosity · Basefluid types · Nanoparticles types

Introduction

The addition of nanoparticles to basefluid, called nanofluid [1], can directly influence the physical properties of fluids such as heat transfer and hydrodynamic properties [2–4]. The use of these materials directly reduces the amount of energy consumed by reducing the heat lost within the heat exchangers in the industry. Similarly, nanofluids can be used in heat exchangers and leads to a significant enhancement in heat transfer rate. This can solve the problem of water consumption and waste production indirectly from large industries such as petrochemicals and refineries [5–9]. The heat exchangers with this approach are designed with a smaller size and weight, which is used in large numbers within the all industries. Moreover, nanofluids cause less friction and corrosion on equipment surfaces in comparison with microparticles-loaded fluids and cause less damage to the canals and pumps [10–12]. In order to cool down micro-electromechanical systems that create high heat flux, narrow channels are used as cooling agents that ordinary fluids cannot be used directly; consequently, nanofluid can be used without producing any significant blockage in channels and they can transfer high heat flux due to their enhanced thermal and hydrodynamic properties [13–16].

Experimental researches are of important for the analysis and validation of analytical and theoretical results obtained for nanofluids' properties. These studies,

✉ Ali Abdollahi
a.abdollahi@pmc.iaun.ac.ir

[1] Department of Mechanical Engineering, Najafabad Branch, Islamic Azad University, Najafabad, Iran

especially on viscosity of nanofluids, provide detailed information about the rheological properties of nanofluids, which can directly influence the amount of heat transfer and power needed for pumping fluids. Extensive research on nanofluids' viscosity has been carried out, and it can be concluded from these findings that several factors including the shape and size of nanoparticles, mass fraction, temperature, surfactants, and the acidity of the basefluid can directly influence the rheological properties as well as nanofluids' viscosity. Following is a summary of the finding obtained by other scholars regarding the effect of various parameters on nanofluids' viscosity and rheological properties.

According to the results obtained from previous studies, it can be concluded that the viscosity and rheological properties of the nanofluids depend on nanoparticles shape and size significantly [17–19]. Nyguan et al. [20] investigated the effect of Al_2O_3 nanoparticle size on viscosity of nanofluids. According to the results, they observed that nanoparticles with mean diameters of 36 and 47 nm exhibited approximately same viscosity [20]. In their other study, they observed that by increasing the volume fraction of nanoparticles from 7 to 9%, the effect of the nanoparticles diameter on the nanofluid viscosity was found to be more significant [20]. He et al. [21] studied the viscosity of distilled water-based nanofluid loaded with TiO_2 nanoparticles. In their experiments, they used nanoparticles with mean diameter of 95 and 145 nm. Their results also showed that with the increase in nanoparticle diameter the viscosity of nanofluids enhances significantly [21].

Extensive research has been carried out on the impacts of nanoparticle loads on viscosity of nanofluid [2, 22–31]. It has been pointed out in these studies that by increasing the volume fraction of nanoparticles the viscosity of the nanofluids increases significantly and a wide range of mechanisms have been presented to explain this effect [2, 22–31]. Parsher et al. [28] showed that the viscosity of the nanofluid changed with the volume fraction of the nanoparticles and showed that with the increase in Al_2O_3 loads in basefluid the viscosity of nanofluid increases tangibly. Das et al. [32] and Putra et al. [33] also showed that with the increase in nanoparticle concentrations, the rheological behavior of Al_2O_3/water nanofluid changed to non-Newtonian fluid and the nanofluid viscosity increases significantly due to the increase in solid content of nanofluid. Duangthongsuk et al. [34] showed that by increasing the volume fraction of nanoparticles from 0.2 to 0.2 vol% at temperatures ranged from 15 to 53 °C the viscosity of TiO_2-loaded nanofluid increased by 4–15% relative to pure water as basefluid.

Chevalier et al. [35] also pointed out in their research that with the increase in the volume fraction of silica nanoparticles in ethanol-based nanofluid the viscosity of nanofluid increases significantly compared to pure ethanol. Schmidt et al. [36] showed that by increasing the volume fraction of aluminum oxide nanoparticles in a wide range of basefluids such as polyolefin, cellulose and isoparaffin, the values of nanofluid viscosity increase and this enhancement was observed in volume fractions ranging from 0.25 to 1 vol%. Chandrasekar et al. [37] showed that with the increment of Al_2O_3 nanoparticles volume fraction from 0.33 to 5 vol% a very significant increase was observed in nanofluid viscosity.

Considering the information provided by other researchers on the viscosity of nanofluids, it is concluded that with the increase in temperature the values of nanofluids viscosity reduce significantly and in the all nanofluids the results follow similar to this trend. Large numbers of reports have presented that the temperature as a major factor influences the physical properties of nanofluids including viscosity, thermal conductivity, heat capacity, and density [25]. With the increase in the nanofluid temperature, the attractive forces between the nanoparticles and the basefluid molecules reduce due to the larger magnitude in Brownian random motion of nanoparticles and this leads to a significant reduction in nanofluid viscosity [38, 39].

Goharshadi et al. studied the rheological properties of zirconium oxide/ethylene glycol nanofluid at different temperatures. They observed that with increasing the temperature the viscosity of nanofluid diminishes. They were also able to estimate viscosity data obtained by experimentation by using the model they proposed [40].

Pastoriza et al. [41] measured the viscosity of alumina/ethylene glycol nanofluids at different temperatures. Their experimental results showed that with the temperature enhancement the nanofluid viscosity decreases, and this declination was according to the following equation:

$$\ln \mu_{\mathrm{nf}} = A + \frac{B}{C + T} \tag{1}$$

Namburu et al. [26] also measured the nanofluid viscosity in a temperature range of 50–35 °C. They observed that by the decrease the temperature viscosity of nanofluid increases, and the rheological behavior of nanofluid approaches non-Newtonian state in case of temperature declination close to the freezing point of the basefluid. Sundar et al. [42] investigated the effect of temperature on nanofluid viscosity containing iron oxide nanoparticles dispersed in distilled water. Their results exhibited that the viscosity of nanofluid depends on temperature significantly, and a large reduction in this parameter was seen by increasing the temperature.

The aim of this study is to study the impacts of both basefluid and nanoparticles types on dynamic viscosity of nanofluid. For this purpose, two types of nanoparticles

were dispersed in aqueous and non-aqueous basefluids separately. Then, the viscosity of nanofluids was measured in different temperatures and nanoparticles' mass fraction. In addition, comprehensive correlations were obtained by using hybrid GMDH-type neural network method for the prediction of nanofluid viscosity at various conditions. Considering the impacts reported in previous researches regarding nanoparticles density on thermophysical properties of nanofluids including dynamic viscosity and thermal conductivity [2, 3, 43, 44], in this research both Al_2O_3 and WO_3 nanoparticles were chosen as an available and commercial nanoparticles, whose densities are 3.95 and 7.16 g cm^{-3}, respectively, for the purpose of accentuating on the influence of this parameter on experimental dynamic viscosity of nanofluids and final proposed correlation at various nanoparticles loads and temperatures. Furthermore, the other factor that increasingly effect the dynamic viscosity of nanoparticles was chosen to be the type of basefluids due to the forces resulted from the polarity of water molecules as well as weak Van Der Waals forces between paraffin molecules [23, 43, 45]. Thus, it is worthwhile to investigate the effect of these intramolecular forces, which can be implied from macroscopic properties of pure basefluids [46], on viscosity of nanofluid containing oxides nanoparticles with different molecular weights.

Experimental

Materials

In this research, Al_2O_3 and WO_3 nanoparticles were purchased from US Nano Company with purity of 99.99%, and physical properties of nanoparticles are presented in Tables 1 and 2, respectively. Moreover, for the preparation of nanofluids, deionized water was used and liquid paraffin model 107160 was purchased from Merck Company, Germany, with detailed physical properties presented in Table 3. In addition, deionized water was used for washing the laboratory glasswares [23].

Instruments

In this study, a cylindrical viscometer (Brookfield model DV2T, USA) was used with detailed specification presented in Table 4 for measuring the viscosity of oxides nanoparticles-loaded nanofluids at condition where various nanoparticles mass fraction was used. For imaging and estimating the size and morphology of nanoparticles, transmission electron microscopy analysis (TEM) (Hitachi, 9000 NA, Japan) was used on de-moisturized nanoparticles. Also for the estimation of Al_2O_3 and WO_3 nanoparticles stability within the deionized water and paraffin model 107160, zeta potential analysis was performed on nanofluids samples containing 0.005 mass% nanoparticles by using the plot of total counts versus total electrostatic voltage (obtained from ZetaSizer, Malvern, ZetaSizer Nano ZS, UK). During the applying viscosity measurement, the temperature was set on constant value by using an isothermal circulator bath (− 40, 7 L Ref. Circulator, PolyScience Co., USA) and for the preparation of stock nanofluid certain amount of Al_2O_3 and WO_3 nanoparticles was measured by using a precise electric balance (HT series, Che Scientific Co., Hong Kong). Finally, in order to measure the sizes of nanoparticles within the aqueous and non-aqueous basefluids and observe the distribution size of nanoparticles, dynamic light scattering (DLS) (Malvern, ZetaSizer Nano ZS, UK) was performed on diluted samples.

Table 1 Physical properties of Al_2O_3 nanoparticles

Molecular weight	101.96 g mol^{-1}
Density	3.95 g cm^{-3}
Melting point	2072 °C
Boiling point	2977 °C

Table 2 Physical properties of WO_3 nanoparticles

Molecular weight	231.84 g mol^{-1}
Density	7.16 g cm^{-3}
Melting point	1473 °C
Boiling point	1700 °C

Table 3 Physical properties of liquid paraffin model 107160

EC no. and CAS no.	232-384-2 and 8012-95-1
Vapor pressure at 20 °C	< 0.01 Pa
Density at 20 °C	0.86 g cm^{-3}
Kinematic viscosity at 40 °C	42.5 mm^2 s^{-1}
Boiling point	300–500 °C
Ignition point	300 °C

Table 4 Specification of viscometer used in this study

Sample volume	5 mL^{-1}
Range of viscosity measurement	1–2,000,000 cp
Accuracy of viscometer	± 1%
Spindle materials	Stainless steel
Maximum temperature operation	190 °C

Nanofluid preparation

In this study, in order to prepare nanofluids with different nanoparticles loads a certain amount of Al_2O_3 and WO_3 nanoparticles was first weighed (about 1 g of oxide nanoparticles) and then dispersed in 19 g of distilled water or liquid paraffin separately under stirring condition of 500 rpm for 30 min. Afterwards, in order to separate the agglomerates of nanoparticles within the basefluids the solutions were placed under sonication waves with a time period of 0.5 s and amplitude of 60% for three steps of 20 min with 5 min rest between each step. Then, other concentrations of nanofluids were made by diluting the stock solution obtained at this stage as given in Table 5.

In order to make solutions with lower concentrations (for example 1 mass%), 4 g of stock nanofluid with a concentration of 5% was taken in accordance with the values presented in Table 5 and then the desired basefluid (water or liquid paraffin) was added to nanofluid until the total mass of nanofluid reaches 20 g. Accordingly, for the preparation of nanofluids with various nanoparticles loads (5, 1, 0.5 and 0.1 mass%), a certain amount of stock colloidal suspension was diluted by adding pure basefluids.

Measuring dynamic viscosity of nanofluids

In order to measure the dynamic viscosity of nanofluid with various mass fractions of oxides nanoparticles in aqueous and non-aqueous basefluids, 5 mL of each sample was introduced to a cylindrical vessel. After putting the spindle of viscometer, the values of shear stress were measured at different shear rates of 2.6, 3.5, 4.8, 6.1, 6.9, 11.8, 14.2, 19.4, 36.0, 53.9, and 64.6 1 s^{-1}. Also the temperature of vessel was kept at 5, 25, 45, and 65 °C, and the viscosity of each sample was measured at different temperatures. In addition for eliminating any further experimental errors and avoid effect of every unstable temperature, the measurements were repeated 2 times at constant condition. Thus, the standard deviation for dynamic viscosity measurement at fixed temperature and nanoparticles mass fraction was calculated by using Eq. 2:

$$\mathrm{SD} = \sqrt{\frac{\sum_{\mathrm{i}} (\mu_{\mathrm{i}} - \bar{\mu})^2}{n^2}} \tag{2}$$

where μ_{i} is dynamic viscosity of nanofluid at fixed shear rate, $\bar{\mu}$ is average dynamic viscosity of nanofluid, and n is numbers of measurements (m = 11 for each asserted shear rate).

Uncertainty analysis

The uncertainty of each measurement was calculated by using dynamic viscosity measurement error, the error of precise electric balance, and isothermal circulator bath error. Thus, according to accuracy of thermal circulator bath (± 0.005 °C), precise electric balance (± 0.0003 g) and the accuracy of viscometer (± 1%), the uncertainty of experimentation was calculated by means of Eq. 3 [47]:

$$\mathrm{UM} = \pm \sqrt{\left(\frac{\Delta\mu}{\mu}\right)^2 + \left(\frac{\Delta w}{w}\right)^2 + \left(\frac{\Delta T}{T}\right)^2} \tag{3}$$

The maximum value of uncertainty for dynamic viscosity measurement was found to be 8.3%.

Results and discussion

Characterization

TEM analysis

In this research, TEM test was used to determine the shape and sizes of dry nanoparticles. In order to apply TEM analysis on samples, aluminum oxide and tungsten oxide nanoparticles were dispersed in ethanol with mass fraction of 0.0001 mass%. Then, the samples were introduced to TEM after full evaporation of ethanol. Figure 1 shows the results of TEM analysis of Al_2O_3 nanoparticles. The results of this figure indicate that mean diameter of Al_2O_3 nanoparticles was found to be 40 nm, mostly ranged from 10 to 70 nm. In addition, it is evident from the results of TEM analysis that the Al_2O_3 nanoparticles morphology was spherical.

Table 5 Mass of stock nanofluid needed for the preparation of diluted nanofluids

Nanofluid mass fraction in basefluid/mass%	Mass of nanofluid taken from stock solution/g	Final mass of nanofluid after dilution/g
5	–	20
1	4	20
0.5	2	20
0.1	0.4	20

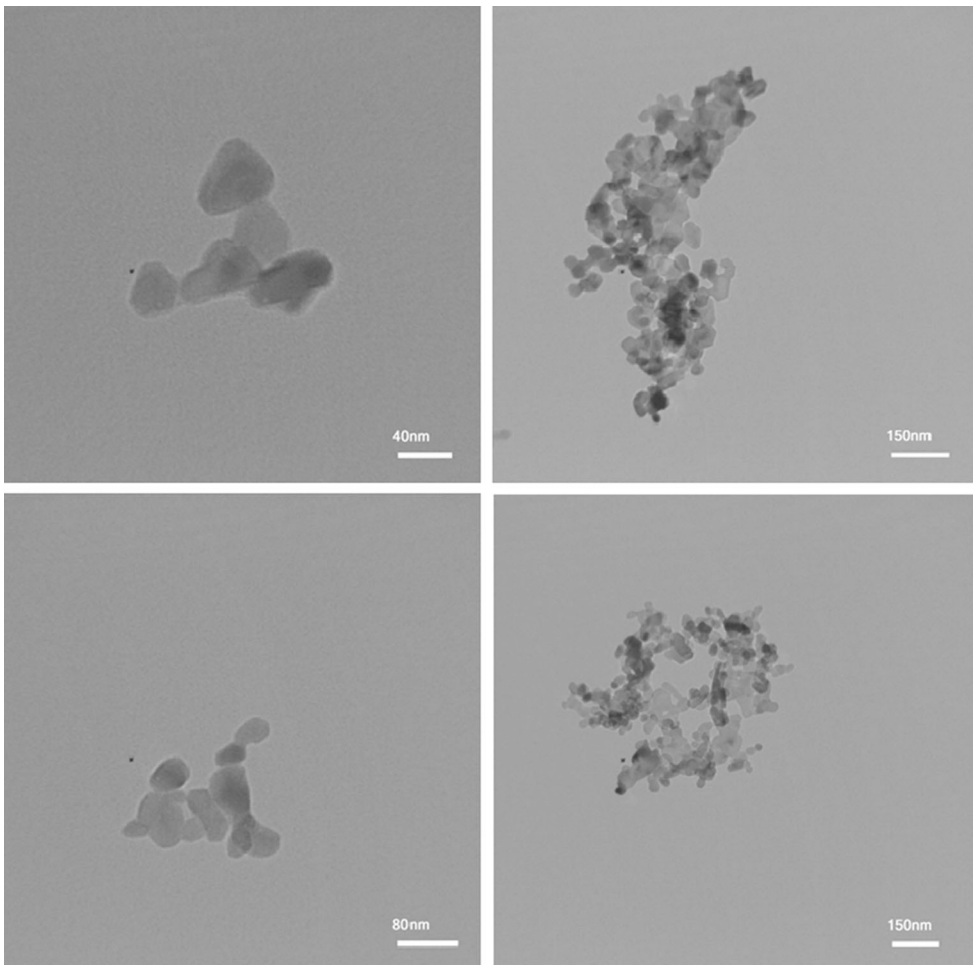

Fig. 1 TEM images of Al_2O_3 nanoparticles

Figure 2 also shows the results of TEM analysis of WO_3 nanoparticles. The results of this figure exhibit that mean diameter of WO_3 nanoparticles was found to be nearly 20 nm, mostly ranged from 10 to 40 nm. This figure also shows that the WO_3 nanoparticles morphology was spherical similar to those obtained for Al_2O_3 nanoparticles. According to the results of previous efforts, that nanoparticle shape has highest impact on hydrodynamic properties of nanofluid [2, 3, 23, 44]. It is concluded from the results of Figs. 1 and 2 that both Al_2O_3 and WO_3 have spherical morphology; therefore, the difference on nanofluids' viscosity may not be resulted from shape and morphology of nanoparticles.

DLS analysis

In this research, dynamic light scattering (DLS) was used for measuring the mean diameter of Al_2O_3 and WO_3 as well as distribution curve for nanoparticles' size in basefluids (distilled water and liquid paraffin model 107160). The results of DLS analysis for each nanofluids sample are shown in Fig. 3. The results of DLS analysis for Al_2O_3/water and Al_2O_3/liquid paraffin show that the average diameter of the nanoparticles in both basefluids (after applying the ultrasonic process) is about 42 nm (Fig. 3a, b), and the polydispersity index (PDI) for nanoparticles' size in water and liquid paraffin is about 0.342 and 0.412, respectively.

Also, the results of DLS for WO_3/water and WO_3/liquid paraffin (Fig. 3c, d) show that the average size of nanoparticles in the basefluids is about 21 nm and the value of PDI for nanoparticles' size in the water and liquid paraffin is about 0.147 and 0.330, respectively. The results of this analysis show that the average size of nanoparticles is according to those obtained from TEM analysis declaring no significant agglomeration of nanoparticles in basefluids environment.

The stability of colloidal suspension can be measured by using the results of zeta potential analysis [3]. The magnitude and maximum value of zeta potential show the intensity of distributed electrostatic repulsion covered nanoparticles' surface dispersed in basefluid. Consequently, the enhancement in the value of zeta potential more than + 40 mV or less than − 40 mV, depending on

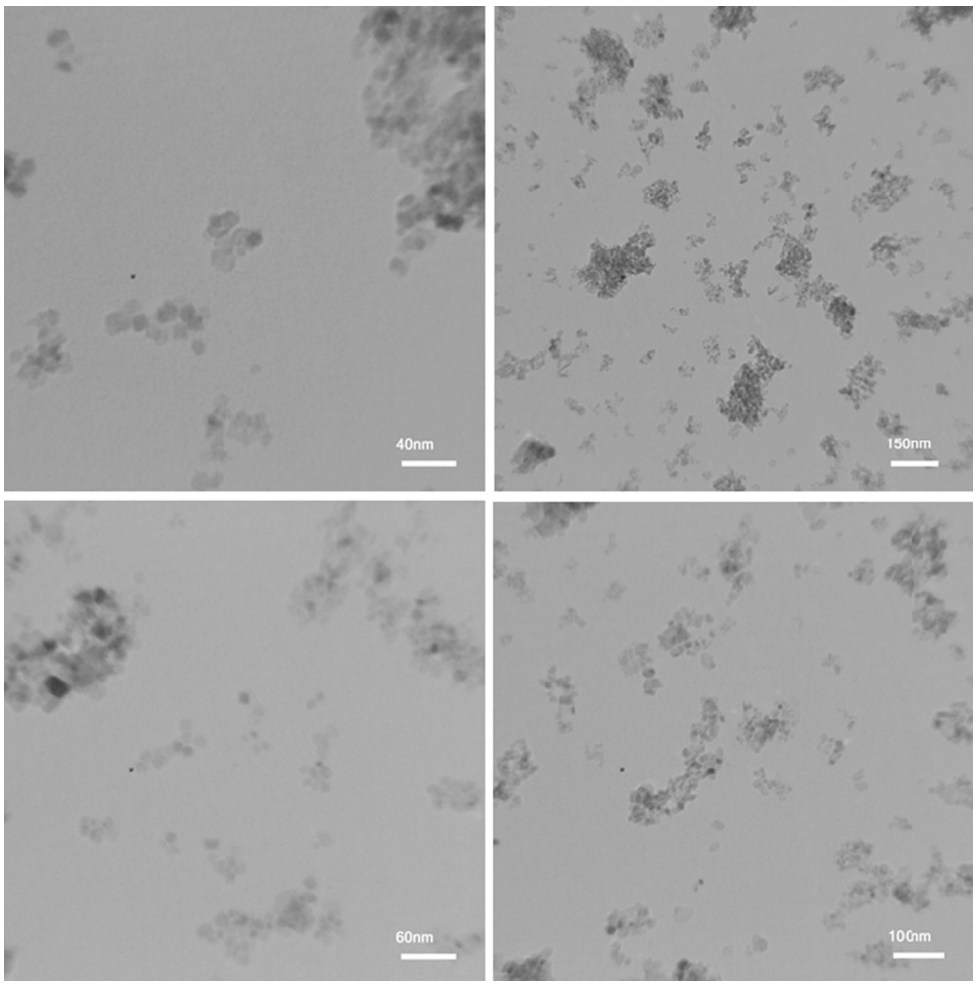

Fig. 2 TEM images of WO_3 nanoparticles

nanoparticles and basefluid type, more stable colloidal suspension are resulted; therefore, larger magnitude of the zeta potential exhibits the higher repulsive electrostatic forces of nanoparticles that do not tend to agglomerate [2, 3, 23, 48, 49].

The results of zeta potential analysis for Al_2O_3/water, Al_2O_3/liquid paraffin, WO_3/water, and WO_3/liquid paraffin are presented in Fig. 4. These results exhibit that the large number of both Al_2O_3 and WO_3 nanoparticles has maximum zeta potential at electrical potential less than − 40 mV, showing high stability of oxides nanoparticles within aqueous and non-aqueous basefluids [2, 50].

Viscosity

In this research, after the preparation of Al_2O_3/water and WO_3/water nanofluids the viscosity of nanofluids was measured at various temperatures and nanoparticles mass fractions. In this case, the mass fraction of nanoparticles was considered as 0.1, 0.5, 1, and 5 mass% and temperature was set on 5, 25, 45, and 65 °C during every measurements. For this purpose, the effects of mentioned parameters were investigated on dynamic viscosity of nanofluids at different strains. Figure 5 shows the value of viscosity versus shear rate for Al_2O_3/water and WO_3/water nanofluid at different temperatures, respectively, and mass fractions of 0.1 and 5 mass%.

As shown in Fig. 5a, b, the viscosity can be considered as a function of the mass fraction of Al_2O_3 nanoparticles at constant temperature and it is evident that with the increase in nanoparticles mass fraction the value of nanofluid dynamic viscosity increases significantly. Also, when Al_2O_3 nanoparticle is added to water the viscosity is measured to be constant in different shear rate declaring Newtonian behavior of nanofluid. Figure 5a, b shows that the viscosity of the nanofluid decreases with increasing temperature, and the value of viscosity deviate at higher temperature resulted in impact of temperature on nanoparticles' random movement. Nano-sized particles have a microscopic effect on hydrodynamic and thermal properties of nanofluid; therefore, according the results obtained by Koo et al. [4] with the temperature increases, the nanoparticle movements and the velocity of these

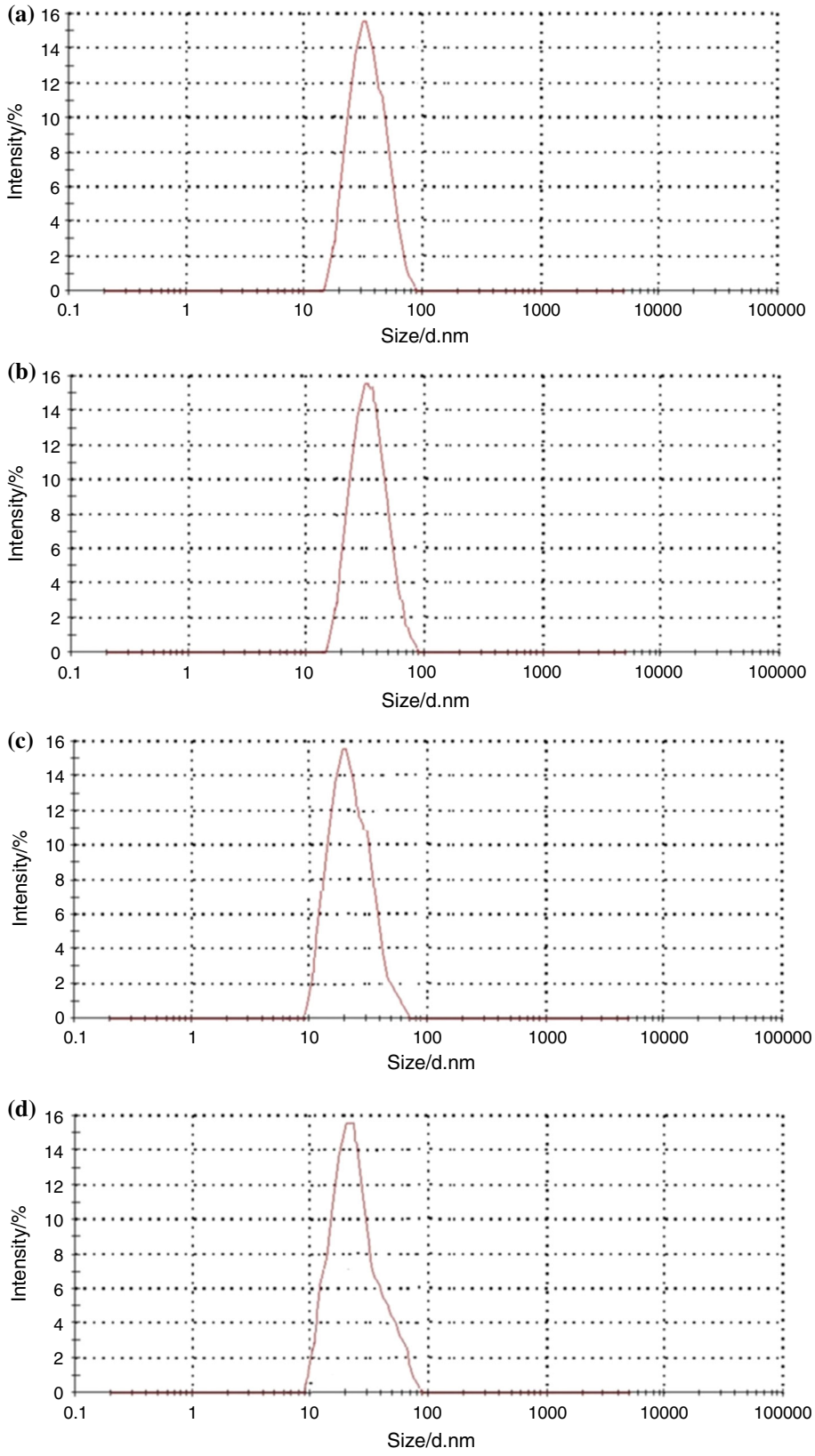

Fig. 3 Results of DLS analysis for **a** Al_2O_3/water, **b** Al_2O_3/liquid paraffin, **c** WO_3/water, and **d** WO_3/liquid paraffin

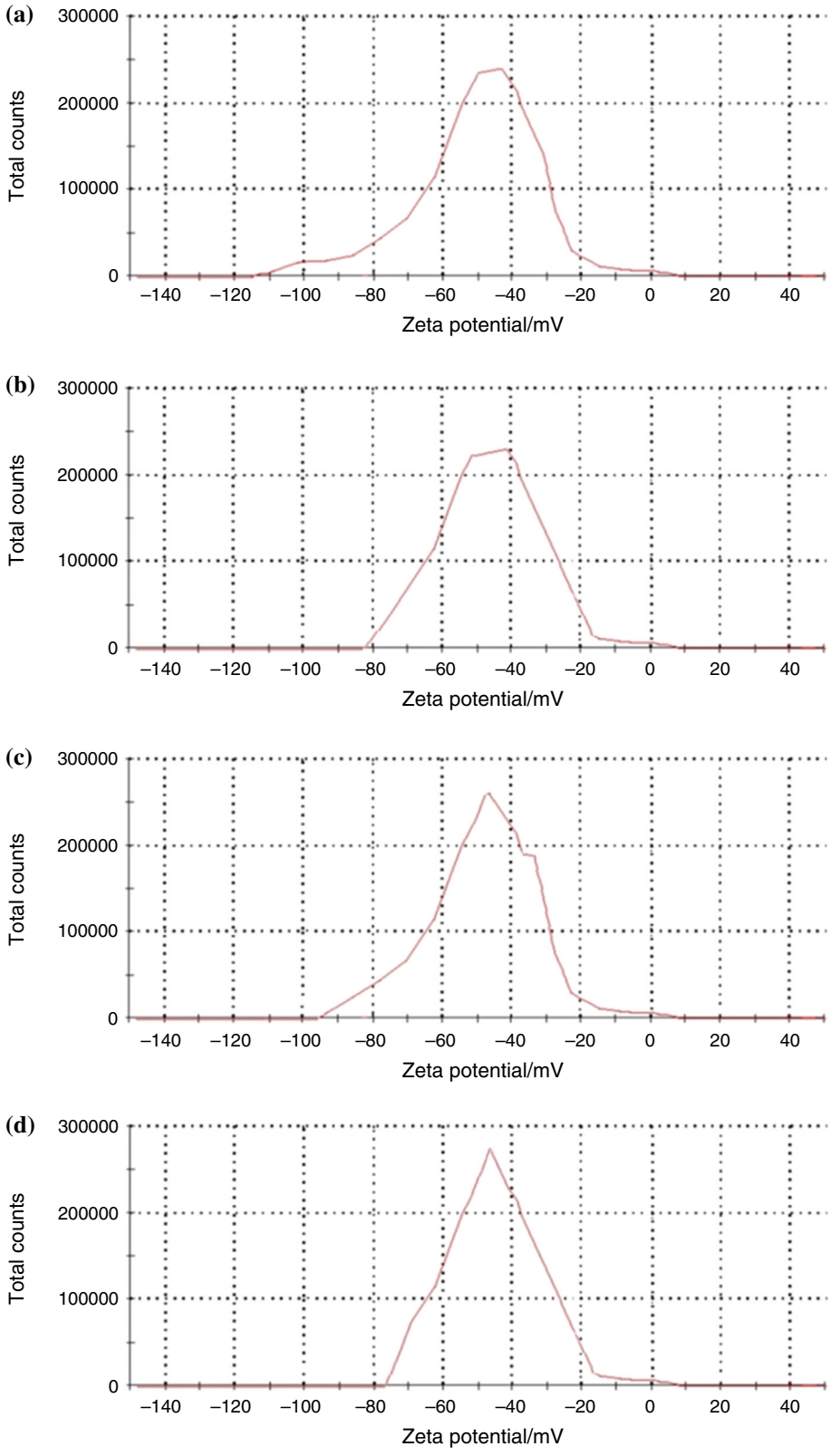

Fig. 4 Results of zeta potential analysis for **a** Al_2O_3/water, **b** Al_2O_3/liquid paraffin, **c** WO_3/water, and **d** WO_3/liquid paraffin

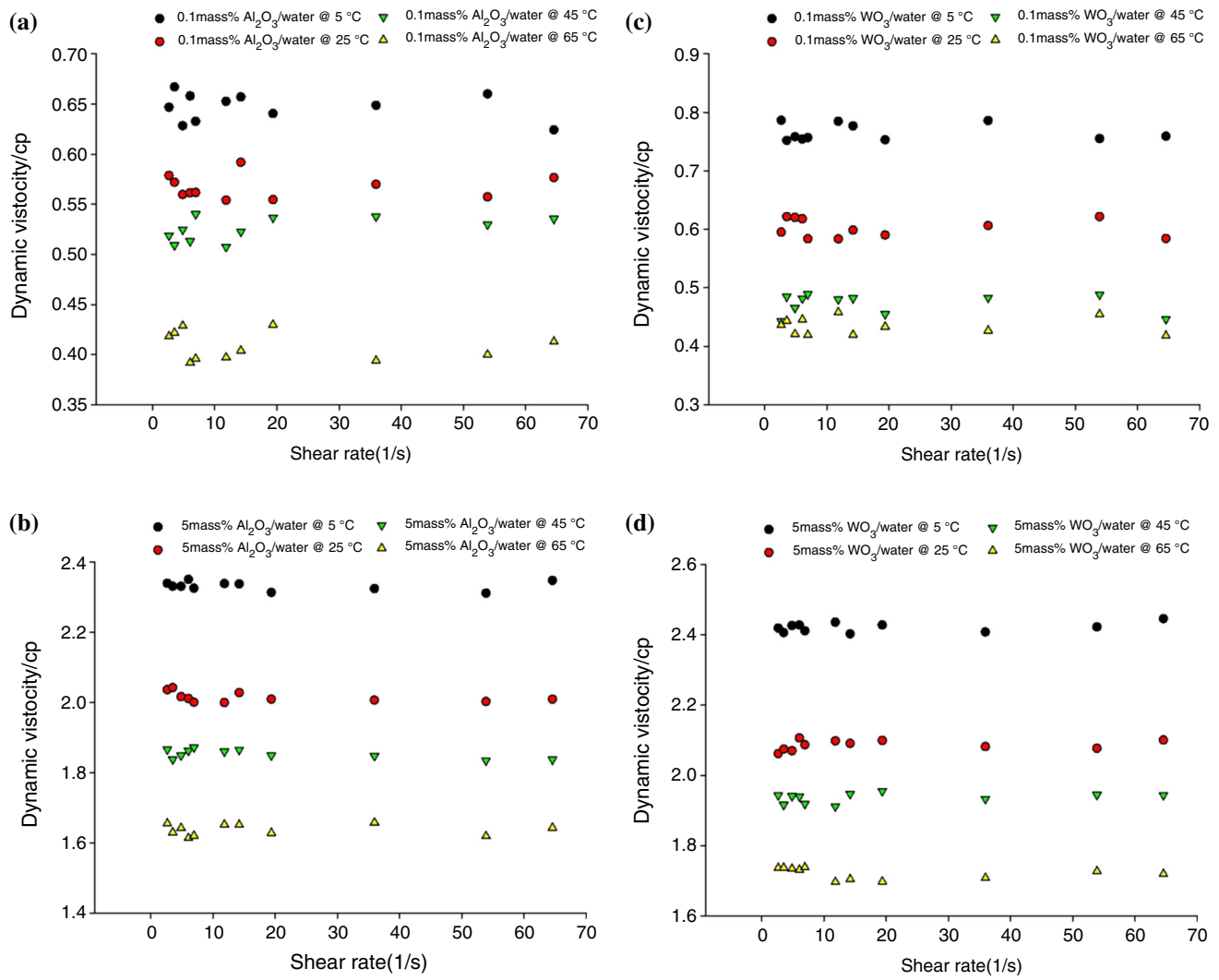

Fig. 5 Dynamic viscosity of Al_2O_3/water at **a** 0.1 and **b** 5 mass% and WO_3/water at **c** 0.1 and **d** 5 mass% of nanoparticles versus shear rate

movements increase leading to higher momentum transfer between fluids' layers.

Figure 5c, d shows the results of measurement for the viscosity of WO_3/water nanofluid versus shear rate at a constant nanoparticles mass fraction and temperature. It can be concluded from this figures that with the increase in nanoparticles mass fraction the value of nanofluid dynamic viscosity increases significantly similar to that obtained for Al_2O_3/water nanofluid, and the value of dynamic viscosity is found to be constant in different shear rate presenting Newtonian behavior of WO_3/water nanofluid. The results presented in Fig. 5c, d exhibit that the viscosity of the nanofluid decreases with increasing temperature due to the enhanced nanoparticles' velocity, leading to declination in intramolecular forces within the basefluid.

Figure 6a, b shows the results of measured dynamic viscosity for Al_2O_3/liquid paraffin nanofluid versus various shear rates at constant temperature and nanoparticles mass fraction. These results exhibit that with the increase in temperature the value of dynamic viscosity declines significantly, and also for the case where nanoparticles are added to liquid paraffin, the viscosity gains higher values at lower shear rate magnitude, indicating the non-Newtonian behavior of Al_2O_3/liquid paraffin nanofluid. These results also show that with the increase in temperature the dependency of nanofluid viscosity to shear rate declines, indicating the Newtonian behavior of nanofluid at higher temperature. In addition, the findings presented in this figures also declare that with the increase in shear rate the value of dynamic viscosity approaches a constant value which is considered as final dynamic viscosity for non-aqueous-based nanofluid in this research.

Figure 6c, d also shows the results of dynamic viscosity for WO_3/liquid paraffin nanofluid versus various shear rates at constant temperature and nanoparticles mass fractions of 0.1 and 5 mass%. These results also show that with

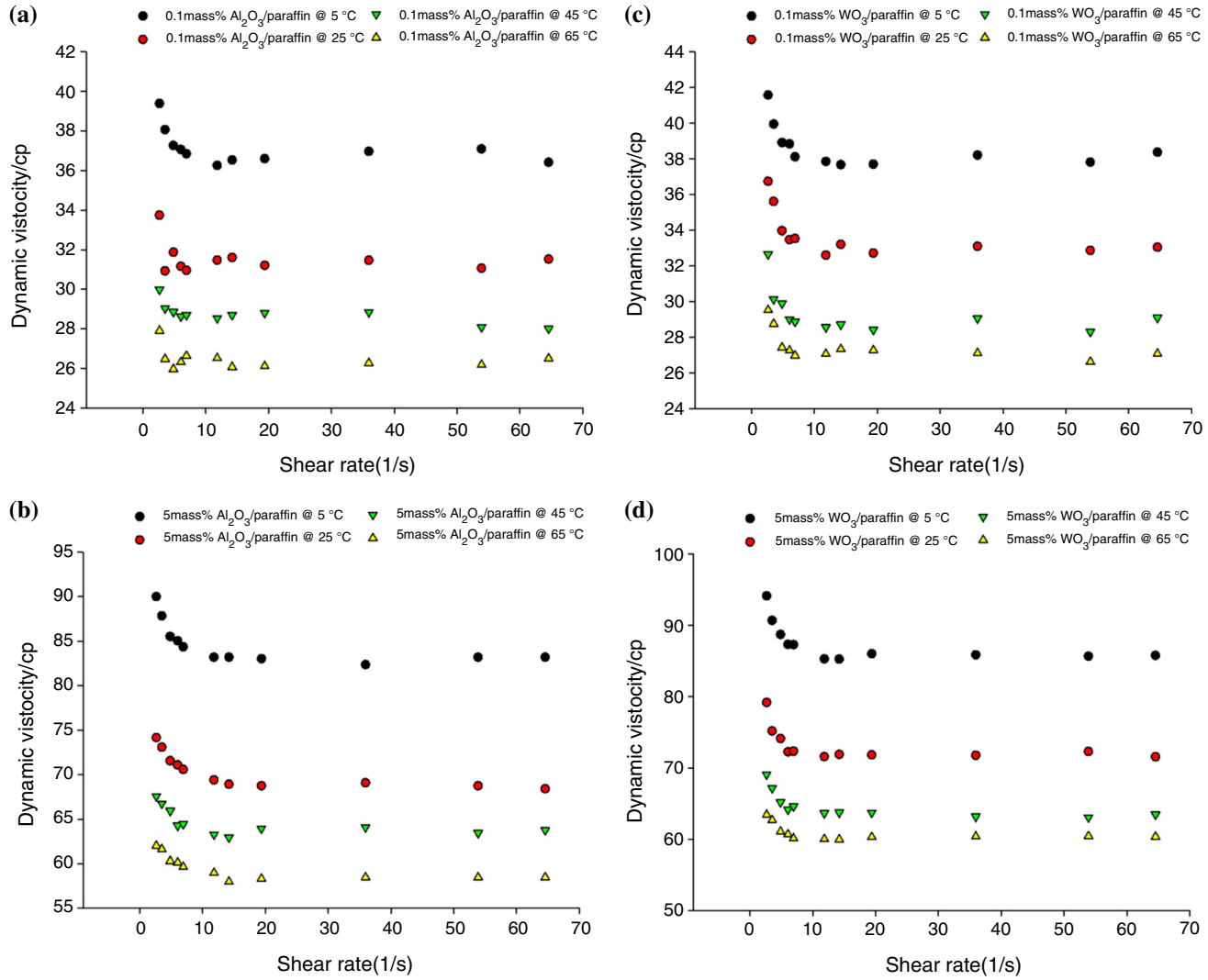

Fig. 6 Dynamic viscosity of Al_2O_3/liquid paraffin at **a** 0.1 and **b** 5 mass% and WO_3/liquid paraffin at **c** 0.1 and **d** 5 mass% of nanoparticles versus shear rate

the increase in temperature the value of dynamic viscosity declines and the value of viscosity is higher at lower shear rate magnitude declaring the non-Newtonian behavior of WO_3/liquid paraffin nanofluid. These results also show that with the increase in temperature the impacts of shear rate on dynamic viscosity decline similar to those obtained for Al_2O_3/liquid paraffin nanofluid and with the increase in shear rate the value of dynamic viscosity approaches a constant value.

Data presented in Fig. 7 show the dynamic viscosity of Al_2O_3/water at various temperatures and nanoparticles mass fractions. These results present that with the increment in nanoparticles mass fraction from 0.1 to 5 mass% the dynamic viscosity of nanofluid increases from 1.6 to 2.3 Pa.s at fixed temperature of 5 °C. In addition, with the increase in nanoparticles load from 0.1 to 5 mass% the dynamic viscosity of nanofluid enhances from 0.4 to

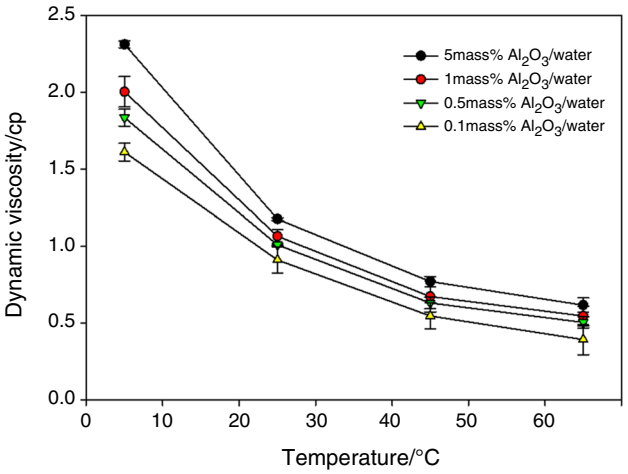

Fig. 7 Dynamic viscosity of Al_2O_3/water nanofluid at different temperatures and mass fractions

0.7 Pa.s at 65 °C. According to the results presented in this figure, it is evident that for Al_2O_3/water the increase in the temperature leads to significant declination in nanofluid dynamic viscosity. Consequently, with temperature enhancement from 5 to 65 °C the value of average dynamic viscosity reduces around 75% for those contain 0.1 mass% Al_2O_3 nanoparticles; however, for the condition where the mass fraction was set on 5 mass% this enhancement in temperature leads to dynamic viscosity declination about 69%. It can be observed from the results of this figure that both temperature and nanoparticles mass fraction have intense impact on the dynamic viscosity of Al_2O_3/water nanofluid, although it has been reported [2, 3, 44, 51] that the temperature influences the hydrodynamic and thermal properties of nanofluid more intensively.

Figure 8 exhibits the dynamic viscosity of Al_2O_3/liquid paraffin at various temperatures and nanoparticles mass fractions. These results also show that with the increase in nanoparticles mass fraction from 0.1 to 5 mass% the value of dynamic viscosity enhances from 58 to 93 Pa.s at temperature of 5 °C and with the increase in Al_2O_3 nanoparticles mass fraction from 0.1 to 5 mass% the dynamic viscosity of nanofluid enhances from 25 to 32 Pa.s at 65 °C. According to the results presented in this figure, it is evident that with the increase in temperature from 5 to 65 °C the value of average dynamic viscosity decreases around 57% for 0.1 mass% Al_2O_3/water nanofluid. However, for the condition where the mass fraction was set on 5 mass% this enhancement in temperature leads 54% declination in dynamic viscosity of nanofluid.

The results presented in Fig. 9 show the measured dynamic viscosity of WO_3/water nanofluid at various temperatures and nanoparticles loads. These results represent that with the increase in nanoparticles mass fraction from 0.1 to 5 mass% the value of average dynamic viscosity of water-based nanofluid increases from 1.7 to 2.4 Pa.s at temperature of 5 °C and with the increase in nanoparticles load from 0.1 to 5 mass% the value of this parameter enhances from 0.4 to 0.8 Pa.s at 65 °C. The results of this figure also show that with the increase in temperature from 5 to 65 °C the value of average dynamic viscosity reduces around 76% for 0.1 mass% WO_3/water nanofluid, although for nanofluid with nanoparticles mass fraction of 5 mass% this enhancement in temperature causes 67% decrease in dynamic viscosity of WO_3/water nanofluid.

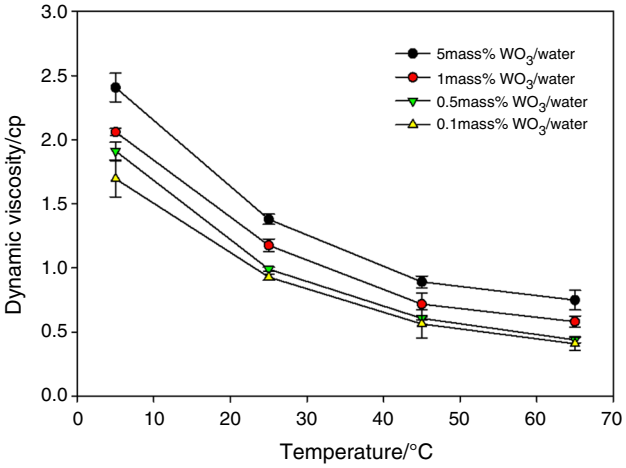

Fig. 9 Dynamic viscosity of WO_3/water nanofluid at different temperatures and mass fractions

The results of dynamic viscosity measurement WO_3/liquid paraffin nanofluid are presented in Fig. 10 versus various temperatures at various WO_3 nanoparticles mass fractions. These results clearly show that with the enhancement in WO_3 nanoparticles mass fraction in liquid paraffin from 0.1 to 5 mass% the value of nanofluid

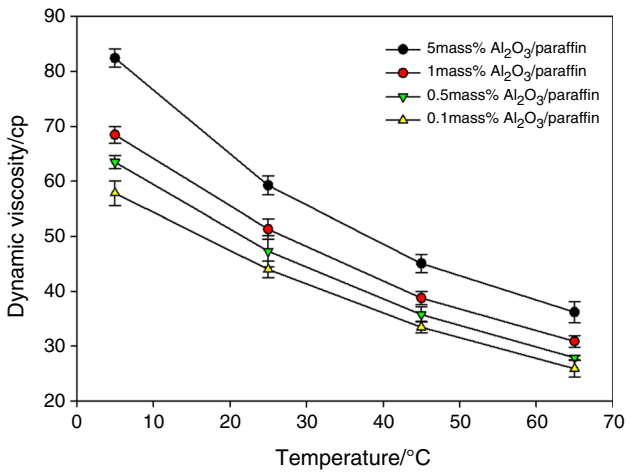

Fig. 8 Dynamic viscosity of Al_2O_3/liquid paraffin nanofluid at different temperatures and mass fractions

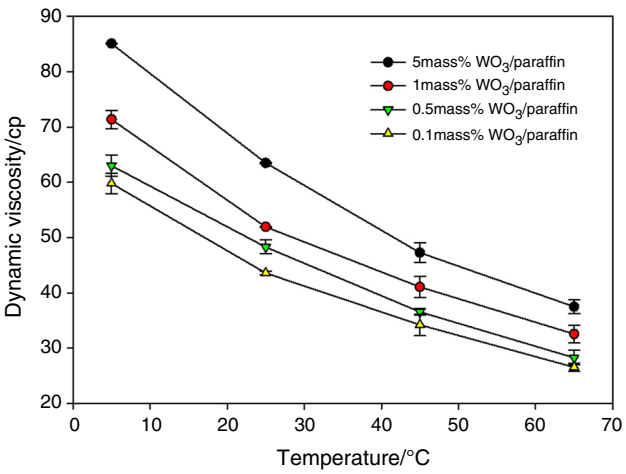

Fig. 10 Dynamic viscosity of WO_3/liquid paraffin nanofluid at different temperatures and mass fractions

dynamic viscosity increases from 60 to 85 Pa.s at 5 °C and for the same enhancement in nanoparticles mass fraction the value of this parameter enhances from 26 to 39 Pa.s at 65 °C. According to results of this figure, it can be concluded that with the increase in temperature from 5 to 65 °C the value of average dynamic viscosity reduces around 53% for nanofluid containing 0.1 mass% WO_3 nanoparticles and for those nanofluids containing 5 mass% nanoparticles the enhancement in temperature from 5 to 65 °C leads 54% decrease in dynamic viscosity of WO_3/liquid paraffin nanofluid.

Effect of temperature

The experimental results of this study show that with the increase in temperature the viscosity of oxides nanoparticles-loaded nanofluid declines independent to basefluid types. The main mechanism for this declination is due to the induced micro-convection caused by random motion of nanoparticle leading to a significant decrease in intermolecular forces between basefluid components [2, 4, 52]. The results of this study showed that with the increase in temperature as shown in Figs. 7–10 for Al_2O_3/water, Al_2O_3/liquid paraffin, WO_3/water, and WO_3/liquid paraffin nanofluids the dynamic viscosity decreases significantly. In addition, it is concluded from the results of this study that with the increase in temperature from 5 to 65 °C the maximum value of dynamic viscosity reduction (76%) was obtained for WO_3/water nanofluid with nanoparticles mass fraction of 0.1 mass%, although the minimum value of viscosity declination (53%) was achieved for WO_3/liquid paraffin nanofluid with nanoparticles mass fraction of 0.1 mass%.

Effect of nanoparticles mass fraction

In addition, the results presented in Figs. 7–10 declared that with the increase in mass fraction of oxides nanoparticles within the aqueous and non-aqueous basefluids the dynamic viscosity of nanofluids increases due to the enhancement in solid nanoparticles content. The results of this study also declared that with the increase in the mass fraction of Al_2O_3 and WO_3 nanoparticles from 0.1 to 5 mass% at the temperatures of 5, 25, 45, and 65 °C the dynamic viscosity of Al_2O_3/liquid paraffin nanofluid increases about 31, 28, 27, 36% and for WO_3/liquid paraffin nanofluid this enhancement was found to be 38, 34, 28, and 30%, respectively.

Effect of basefluid and nanoparticles types

Figure 11 shows the value of dynamic viscosity at various temperatures and nanoparticles mass fraction of 5 mass%.

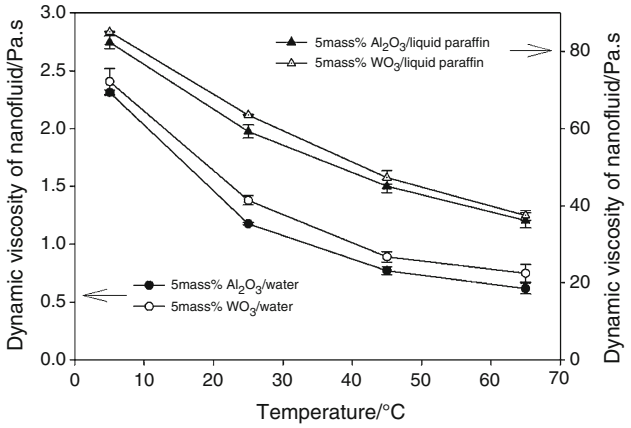

Fig. 11 Dynamic viscosity of nanofluids at different temperatures and nanoparticle mass fraction of 5 mass%

These results indicate that for nanofluids with same basefluid (water or liquid paraffin), WO_3 nanoparticles increases the viscosity of nanofluid more that Al_2O_3 nanoparticles. According to the Brownian motion of nanoparticles, it has been indicated that with the increase in nanoparticles density the velocity magnitude of nanoparticles random motion decreases [2, 3, 44]; therefore, for this case it is concluded that due to the higher density of WO_3 nanoparticles in comparison with Al_2O_3 nanoparticles higher dynamic viscosity is expected.

Also it is evident from the results of Fig. 11 that for nanofluids with different basefluids, similar effect of nanoparticles' type is observed. Accordingly, for both aqueous- and non-aqueous-based nanofluids, addition of WO_3 increases the viscosity of nanofluid more than that contains Al_2O_3 nanoparticles. Therefore, it is concluded that nanoparticles type has much higher impact on nanofluid viscosity in comparison with basefluid type and this effect would be independent of basefluid types.

In this research, the rheological behavior of nanofluid, obtained from experimental data, exhibit that paraffin-based nanofluid shows shear-thinning behavior which strongly depends on several parameters including nanoparticles shape and size, nanoparticles mass fraction, and temperature. According to previous efforts, it is mentioned that with the increase in shear rate aggregated nanoparticles give up the intermolecular forces that lead to make nanoparticles together. By this external force, these aggregates lunch to break apart and consequently move in the direction in which shear rate increases, resulting a significant decrease in viscosity of the nanofluid [53]. Furthermore, with the increase in the shear rate the viscosity of nanofluids approaches a constant value representing weak interactions between nanoparticles. On the contrary, with the declination in shear rate a significant growth of nanoparticles forms and causes to rebuild a

strong network which resist against any external forces [53]. In this research, non-Newtonian behavior of paraffin-based nanofluids at low shear rates is similar to those of observed by previous researcher with implementation of different nanoparticles [21, 53–55].

Correlation

Aqueous-based nanofluid

In this research for estimating the relative dynamic viscosity of water-based nanofluids at various temperature and oxides nanoparticles mass fractions, a regression analysis was made based on hybrid group method of data handling (GMDH)-type neural network [22]. Therefore, a correlation for calculating relative dynamic viscosity of Al_2O_3/water and WO_3/water nanofluid was obtained as function of temperature (°C), nanoparticles and basefluid physical properties (λ), and nanoparticles' mass fraction (mass%), by using GMDH Shell DS software (the following correlation was obtained with $R^2 = 0.97$):

$$\frac{\mu_{nf}}{\mu_b} = \frac{B_1\lambda^a + B_2T^b + B_3w^c + B_4}{1.5447e^{-0.023.T}}$$
$$B_1 = -1.228, \quad B_2 = -3.027, \quad B_3 = 0.575,$$
$$B_4 = 6.256, \quad a = -0.206, \quad b = 0.130, \quad c = 0.192 \tag{4}$$

where

$$\lambda = \frac{Mw_{np}\rho_{np}}{Mw_{bf}\rho_{bf}} \tag{5}$$

where Mw_{np} and ρ_{np} are molecular weight and density of nanoparticles and Mw_{bf} and ρ_{bf} are also molecular weight and density of basefluid (water). Adding nanoparticles increases the viscosity of nanofluid. In addition, with the decrease in shear rate, at constant temperature and nanoparticles mass fraction, higher viscosity is resulted for liquid paraffin-based nanofluids; therefore, it is convenient to used average dynamic viscosity of nanofluid for prediction of appropriate correlation at which this parameter approaches to a constant value, (for viscosity measurement at shear rates of higher than 10 L s^{-1}).

Figure 12 shows the value of relative dynamic viscosity of nanofluid which have been obtained by Eq. 4 versus experimental values of relative dynamic viscosity for Al_2O_3/water and WO_3/water nanofluids. It is evident from the results of this figure that Eq. 4 can estimate the ratio of dynamic viscosity of water-based nanofluid to pure basefluid at various temperatures of 5, 25, 45, and 65 °C and nanoparticle mass fractions of 0.1, 0.5, 1, and 5 mass% for Al_2O_3/water and WO_3/water nanofluids with deviation majorly less than 10% from experimental values.

Non-aqueous-based nanofluid

Also in order to estimate the relative dynamic viscosity of liquid paraffin-based nanofluids at various temperature and nanoparticles mass fractions, a regression analysis was made based on (GMDH)-type neural network [22]. For this purpose, a correlation for the estimation of the dynamic viscosity of Al_2O_3/liquid paraffin and WO_3/liquid paraffin nanofluid was obtained incorporating temperature (°C), nanoparticles and basefluid physical properties ($\acute{\lambda}$), and nanoparticles' mass fraction (mass%) with $R^2 = 0.96$:

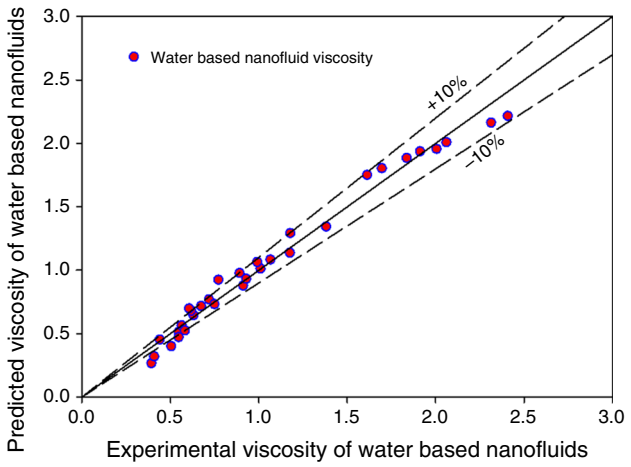

Fig. 12 Relative dynamic viscosity obtained by Eq. 4 versus experimental values

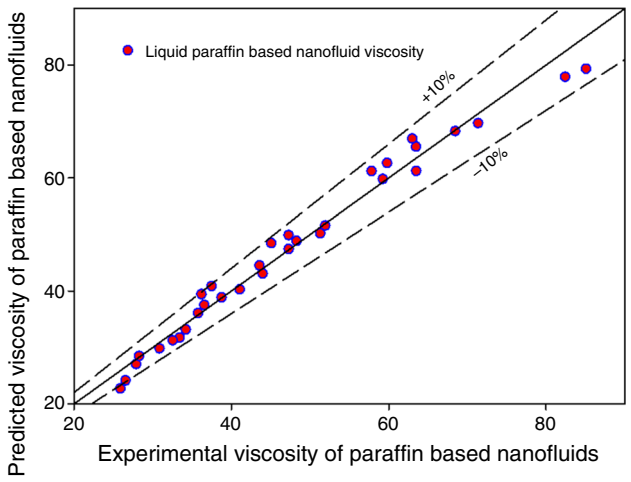

Fig. 13 Relative dynamic viscosity obtained by Eq. 6 versus experimental values

Table 6 Comparison between data obtained by Eqs. 3 and 6 with experimental data for Ag/ethylene glycol nanofluid viscosity

Temperature/ °C	λ	Mass fraction/mass%	Experimental data	Data obtained by Eq. 3	Data obtained by Eq. 6	Deviation of values obtained by Eq. 3 from experimental data	Deviation of values obtained by Eq. 6 from experimental data
40	16.4	8.72	1.45	2.51	1.86	− 73.39	− 28.72
45	16.4	8.72	1.45	2.68	1.81	− 85.04	− 24.55
50	16.4	8.72	1.52	2.87	1.75	− 88.83	− 15.05
45	16.4	6.67	1.34	2.60	1.72	− 94.29	− 28.95
50	16.4	6.67	1.41	2.87	1.67	− 97.22	− 18.48
40	16.4	4.54	1.24	2.34	1.68	− 89.31	− 35.78
45	16.4	4.54	1.25	2.50	1.62	− 99.68	− 29.85
50	16.4	4.54	1.28	2.66	1.56	− 107.84	− 22.33
45	16.4	2.32	1.10	2.33	1.45	− 111.51	− 32.50
50	16.4	2.32	1.12	2.47	1.40	− 120.55	− 25.04

Table 7 Comparison between data obtained by Eqs. 3 and 6 with experimental data for NiO/crude oil nanofluid viscosity

Temperature/ °C	λ	Mass fraction/mass%	Experimental data	Data obtained by Eq. 3	Data obtained by Eq. 6	Deviation of values obtained by Eq. 3 from experimental data	Deviation of values obtained by Eq. 6 from experimental data
40	0.72	2	1.24	1.15	1.21	7.83	3.18
50	0.72	2	1.18	1.16	1.15	1.32	5.18
80	0.72	2	0.97	1.04	0.87	− 6.84	− 10.57

$$\frac{\mu_{\mathrm{nf}}}{\mu_{\mathrm{b}}} = \frac{A_1 \acute{\lambda}^{\acute{a}} + A_2 T^{\acute{b}} + A_3 w^{\acute{c}} + A_4}{52.36 e^{-0.013.\mathrm{T}}}$$
$$A_1 = -32.072, \quad A_2 = -6.191, \quad A_3 = 12.895,$$
$$A_4 = 116.64, \quad \acute{a} = 0.136, \quad \acute{b} = 0.513, \quad \acute{c} = 0.346 \tag{6}$$

where

$$\acute{\lambda} = \frac{M w_{\mathrm{bf}} \rho_{\mathrm{bf}}}{M w_{\mathrm{np}} \rho_{\mathrm{np}}}, \quad \acute{\lambda}\lambda = 1 \tag{7}$$

Figure 13 presents the values of relative dynamic viscosity of nanofluid which have been obtained by Eq. 6 versus experimental values of relative dynamic viscosity obtained for Al_2O_3/liquid paraffin and WO_3/liquid paraffin nanofluids. It is concluded from the results presented in this figure that Eq. 6 can estimate the ratio of dynamic viscosity of liquid paraffin-based nanofluid to those obtained for basefluid at various temperatures of 5, 25, 45, and 65 °C and nanoparticle mass fractions of 0.1, 0.5, 1, and 5 mass% with deviation majorly less than 10% from experimental data.

In order to validate the presented correlation for water-based and liquid paraffin-based nanofluids, experimental data were obtained from previous researches and a comparison was made on obtained results given in Table 6. According to the results presented in this table, experimental data were obtained from a research (Zadeh et al. [31]), on dynamic viscosity of nano-silver/ethylene glycol nanofluid and the corresponding values were obtained by using Eqs. 3 and 5. It is evident from the results presented in this figure, for the case of nano-silver/ethylene glycol nanofluid Eq. 3 calculates the relative dynamic viscosity of the mentioned nanofluid with a large deviation from experimental value (around 100%), indicating that this correlation cannot estimate the relative dynamic viscosity of nanometal-loaded nanofluid well. Moreover, the data in this table clearly exhibit that Eq. 6 can estimate relative viscosity of mentioned nanofluid with a deviation less than 35%. These results also show that Eq. 6 can predict relative dynamic viscosity of nanofluid within the temperature range of 40–50 °C and nanoparticles' mass fractions of 8.72, 6.67, 4.54, and 2.32 mass% with the least deviation from the experimental data set.

Table 7 also represents the comparison between values obtained by Eqs. 3 and 5 and the experimental data obtained for NiO/crude oil nanofluid viscosity (Attari et al. [2]). It is evident that for the case of NiO/crude oil nanofluid both Eqs. 3 and 5 can estimate nanofluids' viscosity with a deviation less than 10% from the experimental data. These results clearly show that the both correlation can calculate the relative dynamic viscosity of the mentioned nanofluid within the temperature range of 40–80 °C with

NiO nanoparticles mass fraction of 2 mass% within the deviation range of − 10.57 to 7.83.

Conclusions

In this study, the effect of temperature and mass fraction of Al_2O_3 and WO_3 nanoparticles in distilled water and liquid paraffin model 107160, was investigated on dynamic viscosity of nanofluid. In order to prevent agglomeration of nanoparticles during the preparation of nanofluid, they were suspended in aqueous and non-aqueous medium by using an ultrasonic processor.

The results of the TEM tests showed that the size of Al_2O_3 and WO_3 nanoparticles was ranged from 10 to 60 nm, and the results showed that the structure of nanoparticles was semi-spherical. Also the results of DLS and zeta potential tests, respectively, exhibited the size and stability of the nanoparticles in the basefluid environment. In order to carry out viscosity tests, samples of nanofluid including Al_2O_3/water, WO_3/water, Al_2O_3/liquid paraffin, and WO_3/liquid paraffin with mass fractions of 0.1, 0.5, 1, and 5 mass% were prepared and then viscosity tests were performed on samples at 5, 25, 45, and 65 °C.

The results showed that adding a certain amount of nanoparticles to water and liquid paraffin increases viscosity and, in the case of various shear rates, the viscosity is constant for the water-based nanofluids, which indicates the Newtonian behavior of the nanofluid. For those prepared by liquid paraffin as a basefluid, the viscosity is not the same at different shear rates and at low value of shear rate the viscosity is higher, indicating non-Newtonian behavior of liquid paraffin-based nanofluids. Consequently, by adding nanoparticles to the liquid paraffin, the nanofluid behaves like a non-Newtonian fluid at low shear rate values.

Increasing the temperature in liquid paraffin-based nanofluid contributes to the uniformity and linearity of the viscosity curve at various shear rates, which represents Newtonian behavior of nanofluid at higher temperatures. These results showed that with increasing mass fraction of nanoparticles in water and liquid paraffin, the viscosity increases in different shear rates. Finally, the correlation presented in this study shows that for nanofluid viscosity as a function of nanoparticles load and temperature, the deviation of correlated data from experimental values is less than 10%.

References

1. Choi SU-S. Nanofluid technology: current status and future research. Argonne National Lab. (ANL), Argonne, IL (United States); 1998.
2. Attari H, Derakhshanfard F, Darvanjooghi MHK. Effect of temperature and mass fraction on viscosity of crude oil-based nanofluids containing oxide nanoparticles. Int Commun Heat Mass Transfer. 2017;82:103–13.
3. Darvanjooghi MHK, Esfahany MN. Experimental investigation of the effect of nanoparticle size on thermal conductivity of in situ prepared silica–ethanol nanofluid. Int Commun Heat Mass Transfer. 2016;77:148–54.
4. Koo J, Kleinstreuer C. A new thermal conductivity model for nanofluids. J Nanopart Res. 2004;6(6):577–88.
5. Abdollahi A, Salimpour MR. Experimental investigation on the boiling heat transfer of nanofluids on a flat plate in the presence of a magnetic field. Eur Phys J Plus. 2016;131(11):414.
6. Abdollahi A, Salimpour MR, Etesami N. Experimental analysis of magnetic field effect on the pool boiling heat transfer of a ferrofluid. Appl Therm Eng. 2017;111:1101–10.
7. Salimpour MR, Abdollahi A, Afrand M. An experimental study on deposited surfaces due to nanofluid pool boiling: comparison between rough and smooth surfaces. Exp Thermal Fluid Sci. 2017;88:288–300.
8. Taghizadeh-Tabari Z, Heris SZ, Moradi M, Kahani M. The study on application of TiO_2/water nanofluid in plate heat exchanger of milk pasteurization industries. Renew Sustain Energy Rev. 2016;58:1318–26.
9. Yu W, France DM, Routbort JL, Choi SU. Review and comparison of nanofluid thermal conductivity and heat transfer enhancements. Heat Transfer Eng. 2008;29(5):432–60.
10. Azmi W, Sharma K, Sarma P, Mamat R, Anuar S, Rao VD. Experimental determination of turbulent forced convection heat transfer and friction factor with SiO_2 nanofluid. Exp Thermal Fluid Sci. 2013;51:103–11.
11. Chandrasekar M, Suresh S, Bose AC. Experimental studies on heat transfer and friction factor characteristics of Al_2O_3/water nanofluid in a circular pipe under laminar flow with wire coil inserts. Exp Thermal Fluid Sci. 2010;34(2):122–30.
12. Hwang KS, Jang SP, Choi SU. Flow and convective heat transfer characteristics of water-based Al_2O_3 nanofluids in fully developed laminar flow regime. Int J Heat Mass Transf. 2009;52(1–2):193–9.
13. Wen D, Ding Y. Formulation of nanofluids for natural convective heat transfer applications. Int J Heat Fluid Flow. 2005;26(6):855–64.
14. Xuan Y, Li Q. Heat transfer enhancement of nanofluids. Int J Heat Fluid Flow. 2000;21(1):58–64.
15. Xuan Y, Li Q. Investigation on convective heat transfer and flow features of nanofluids. J Heat Transfer. 2003;125(1):151–5.
16. Xuan Y, Roetzel W. Conceptions for heat transfer correlation of nanofluids. Int J Heat Mass Transf. 2000;43(19):3701–7.
17. Jeong J, Li C, Kwon Y, Lee J, Kim SH, Yun R. Particle shape effect on the viscosity and thermal conductivity of ZnO nanofluids. Int J Refrig. 2013;36(8):2233–41.
18. Mahbubul I, Saidur R, Amalina M. Latest developments on the viscosity of nanofluids. Int J Heat Mass Transf. 2012;55(4):874–85.
19. Timofeeva EV, Routbort JL, Singh D. Particle shape effects on thermophysical properties of alumina nanofluids. J Appl Phys. 2009;106(1):014304.
20. Nguyen C, Desgranges F, Roy G, Galanis N, Maré T, Boucher S, et al. Temperature and particle-size dependent viscosity data for

water-based nanofluids–hysteresis phenomenon. Int J Heat Fluid Flow. 2007;28(6):1492–506.
21. He Y, Jin Y, Chen H, Ding Y, Cang D, Lu H. Heat transfer and flow behaviour of aqueous suspensions of TiO_2 nanoparticles (nanofluids) flowing upward through a vertical pipe. Int J Heat Mass Transf. 2007;50(11–12):2272–81.
22. Atashrouz S, Pazuki G, Alimoradi Y. Estimation of the viscosity of nine nanofluids using a hybrid GMDH-type neural network system. Fluid Phase Equilib. 2014;372:43–8.
23. Ghasemi S, Karimipour A. Experimental investigation of the effects of temperature and mass fraction on the dynamic viscosity of CuO-paraffin nanofluid. Appl Therm Eng. 2017;10:1639–48.
24. Masuda H, Ebata A, Teramae K. Alteration of thermal conductivity and viscosity of liquid by dispersing ultra-fine particles. Dispersion of Al_2O_3, SiO_2 and TiO_2 ultra-fine particles. Netsu Bussei. 1993;7:227–33.
25. Mishra PC, Mukherjee S, Nayak SK, Panda A. A brief review on viscosity of nanofluids. Inte Nano Lett. 2014;4(4):109–20.
26. Namburu P, Kulkarni D, Dandekar A, Das D. Experimental investigation of viscosity and specific heat of silicon dioxide nanofluids. Micro Nano Lett. 2007;2(3):67–71.
27. Nguyen C, Desgranges F, Galanis N, Roy G, Maré T, Boucher S, et al. Viscosity data for Al2O3–water nanofluid—hysteresis: Is heat transfer enhancement using nanofluids reliable? Int J Therm Sci. 2008;47(2):103–11.
28. Prasher R, Song D, Wang J, Phelan P. Measurements of nanofluid viscosity and its implications for thermal applications. Appl Phys Lett. 2006;89(13):133108.
29. Sundar LS, Singh MK, Sousa AC. Investigation of thermal conductivity and viscosity of Fe_3O_4 nanofluid for heat transfer applications. Int Commun Heat Mass Transfer. 2013;44:7–14.
30. Yu W, Xie H, Chen L, Li Y. Investigation of thermal conductivity and viscosity of ethylene glycol based ZnO nanofluid. Thermochim Acta. 2009;491(1):92–6.
31. Zadeh AD, Toghraie D. Experimental investigation for developing a new model for the dynamic viscosity of silver/ethylene glycol nanofluid at different temperatures and solid volume fractions. J Therm Anal Calorim. 2018;131:1449–61.
32. Das SK, Putra N, Roetzel W. Pool boiling characteristics of nano-fluids. Int J Heat Mass Transf. 2003;46(5):851–62.
33. Putra N, Roetzel W, Das SK. Natural convection of nano-fluids. Heat Mass Transf. 2003;39(8–9):775–84.
34. Duangthongsuk W, Wongwises S. Measurement of temperature-dependent thermal conductivity and viscosity of TiO_2-water nanofluids. Exp Therm Fluid Sci. 2009;33(4):706–14.
35. Chevalier J, Tillement O, Ayela F. Rheological properties of nanofluids flowing through microchannels. Appl Phys Lett. 2007;91(23):233103.
36. Schmidt AJ, Chiesa M, Torchinsky DH, Johnson JA, Boustani A, McKinley GH, et al. Experimental investigation of nanofluid shear and longitudinal viscosities. Appl Phys Lett. 2008;92(24):244107.
37. Chandrasekar M, Suresh S, Bose AC. Experimental investigations and theoretical determination of thermal conductivity and viscosity of Al2O3/water nanofluid. Exp Therm Fluid Sci. 2010;34(2):210–6.
38. Andrade EdC. A theory of the viscosity of liquids—part II. Lond Edinb Dublin Philos Mag J Sci. 1934;17(113):698–732.
39. Thomas S, Sobhan CBP. A review of experimental investigations on thermal phenomena in nanofluids. Nanoscale Res Lett. 2011;6(1):377.
40. Goharshadi EK, Hadadian M. Effect of calcination temperature on structural, vibrational, optical, and rheological properties of zirconia nanoparticles. Ceram Int. 2012;38(3):1771–7.
41. Pastoriza-Gallego M, Casanova C, Legido JA, Piñeiro M. CuO in water nanofluid: influence of particle size and polydispersity on volumetric behaviour and viscosity. Fluid Phase Equilib. 2011;300(1–2):188–96.
42. Sundar LS, Singh MK, Sousa AC. Investigation of thermal conductivity and viscosity of Fe_3O_4 nanofluid for heat transfer applications. Int Commun Heat Mass Transfer. 2013;44:7–14.
43. Karimipour A, Ghasemi S, Darvanjooghi MHK, Abdollahi A. A new correlation for estimating the thermal conductivity and dynamic viscosity of CuO/liquid paraffin nanofluid using neural network method. Int Commun Heat Mass Transfer. 2018;92:90–9.
44. Darvanjooghi MHK, Pahlevaninezhad M, Abdollahi A, Davoodi SM. Investigation of the effect of magnetic field on mass transfer parameters of CO_2 absorption using Fe_3O_4–water nanofluid. AIChE J. 2017;63(6):2176–86.
45. Afrand M, Najafabadi KN, Akbari M. Effects of temperature and solid volume fraction on viscosity of SiO_2-MWCNTs/SAE40 hybrid nanofluid as a coolant and lubricant in heat engines. Appl Therm Eng. 2016;102:45–54.
46. Treybal RE. Mass transfer operations. New York: McGraw-Hill Book Company; 1980.
47. Teng T-P, Hung Y-H, Teng T-C, Mo H-E, Hsu H-G. The effect of alumina/water nanofluid particle size on thermal conductivity. Appl Therm Eng. 2010;30(14):2213–8.
48. Esmaeili Faraj SH, Nasr Esfahany M, Jafari-Asl M, Etesami N. Hydrogen sulfide bubble absorption enhancement in water-based nanofluids. Ind Eng Chem Res. 2014;53(43):16851–8.
49. Esmaeili-Faraj SH, Nasr Esfahany M. Absorption of hydrogen sulfide and carbon dioxide in water based nanofluids. Ind Eng Chem Res. 2016;55(16):4682–90.
50. W-g Kim, Kang HU, Jung K-m, Kim SH. Synthesis of silica nanofluid and application to CO_2 absorption. Sep Sci Technol. 2008;43(11–12):3036–55.
51. Darvanjooghi MHK, Esfahany MN, Faraj SHE. Investigation of the effects of nanoparticle size on CO_2 absorption by silica–water nanofluid. Sep Purif Technol. 2017. https://doi.org/10.1016/j.seppur.2017.12.020.
52. Koo J, Kleinstreuer C. Impact analysis of nanoparticle motion mechanisms on the thermal conductivity of nanofluids. Int Commun Heat Mass Transfer. 2005;32(9):1111–8.
53. Aladag B, Halelfadl S, Doner N, Maré T, Duret S, Estellé P. Experimental investigations of the viscosity of nanofluids at low temperatures. Appl Energy. 2012;97:876–80.
54. Abareshi M, Goharshadi EK, Zebarjad SM, Fadafan HK, Youssefi A. Fabrication, characterization and measurement of thermal conductivity of Fe_3O_4 nanofluids. J Magn Magn Mater. 2010;322(24):3895–901.
55. Karimi-Nazarabad M, Goharshadi EK, Entezari MH, Nancarrow P. Rheological properties of the nanofluids of tungsten oxide nanoparticles in ethylene glycol and glycerol. Microfluid Nanofluid. 2015;19(5):1191–202.